Spatially periodic deformations in planar and twisted flexoelectric nematic layers

M. Buczkowska* and G. Derfel
Institute of Physics, Lodz University of Technology, ul. Wólczańska 219, 90-924 Łódź, Poland
(Received 7 March 2017; published 26 June 2017)

Electric field induced deformations in twisted and untwisted planar layers of nematic liquid crystals possessing flexoelectric properties were investigated numerically. The spatially periodic deformations, taking the form of parallel stripes, were found to have smaller free energy than the homogeneous deformations. The structures of distorted layers as well as the evolution of deformations during changes of bias voltage were recognized. The role of flexoelectric properties was analyzed. Calculations taking into account the peculiar elastic properties of the bent-core nematics were also performed. In the untwisted planar layers the stripes were parallel to the initial director orientation. In the twisted layers, two different kinds of periodic deformation were distinguished. They had different structures and different directions with respect to the initial director distribution. The results were consistent with existing experimental data.

DOI: 10.1103/PhysRevE.95.062705

I. INTRODUCTION

Thin layers of nematic liquid crystals confined between plane-parallel electrodes are fundamental for construction of displays and other liquid crystal devices [1]. The general principle of operation of liquid crystal displays consists of electric field induced deformations of director orientation. They should be homogeneous, i.e., identical over the whole area of the electrodes. Such deformations may be considered as one dimensional since the director orientation in the distorted layer depends only on the coordinate normal to the layer.

The influence of electric field on director distribution is related to dielectric anisotropy and to flexoelectricity of the nematic material [2,3]. Deformations qualitatively similar to those of a dielectric nature are induced by magnetic field due to anisotropy of diamagnetic susceptibility [3,4]. In the absence of external electric or magnetic fields, the director distribution in the layer results from boundary conditions imposed by aligning coatings deposited on the surfaces of electrodes. Orientation of the director adjacent to the electrodes is determined by unit vectors called anchoring directions or easy axes [5]. The easy axis indicates the orientation which would be adopted spontaneously by the director if it would not be affected by any other interaction. In the so-called twisted nematic cells, the surface interactions induce planar director orientation; i.e., the easy axes are parallel to the electrodes but the easy axis on one electrode makes the angle $\Phi = 90^\circ$ with the easy axis on the other. As a result, the director orientation varies continuously along the normal to the layer; i.e., the structure is twisted by an angle $\Delta\phi$ which depends on the effectiveness of anchoring and is close to 90°. Such a homogeneously twisted layer is basic for commonly used liquid crystal displays [1].

Under suitable circumstances, external electric or magnetic field induces the two-dimensional deformations in which director orientation in the distorted layer depends not only on the coordinate normal to the layer but it also varies along some direction parallel to the layer. The two-dimensional deformations are spatially periodic. They can be seen under a microscope as parallel stripes. From an applicative point of view the stripes are undesirable since they destroy the homogeneous appearance of the area of an excited pixel of a display. The field induced periodic distortions appear also as transient patterns before the static homogeneous deformations arise. The large class of phenomena resulting in periodic patterns is due to electrohydrodynamic instabilities (electroconvection) in nematics containing ions [6].

In some cases, the electric field induced periodic deformations are caused by flexoelectric torques; nevertheless they can arise also without the contribution of flexoelectricity. The comprehensive review of the periodic patterns of various natures is given by Hinov *et al.* [7]. The role of flexoelectricity in patterns formation is described in [8]. The structure and properties of periodic patterns were the subject of many theoretical and numerical studies. The time dependent flexoelectric instabilities in the presence of an alternating electric field were studied theoretically by Krekhov *et al.* [9]. In particular, the competition of flexodomains with electrohydrodynamic instabilities was analyzed. Here we are focused on static deformations occurring in layers with planar boundary conditions.

Deformations of planar nontwisted layers depend on the elastic properties of nematics. For typical ratios of elastic constants, $r = k_{22}/k_{11}$, which usually adopt values between 0.4 and 0.7, the field induced deformations are one dimensional. However, if $r < r_c \approx 0.303$, the periodic distortions arise prior to the homogeneous deformations and are visible as stripes called periodic splay twist (PST) patterns. Such patterns, induced by magnetic field, were observed experimentally in some liquid crystal polymer possessing sufficiently large elastic anisotropy [10]. Various cases of deformations occurring under the action of electric and/or magnetic fields and with various boundary conditions were analyzed theoretically [11–19]. In the layers with twisted director distribution, the patterns called "Y mode" develop, provided that the twist angle Φ is sufficiently small [20]. They are similar to the PST stripes. If the layer is twisted by sufficiently high angle Φ, usually higher than 90°, the periodic deformations called "X mode" arise [20–24]. In order to avoid them in the super-twisted nematic displays (in which Φ reaches, for instance, 240°), sufficiently large surface tilt angles between easy axes and electrodes are applied [25–27].

*mbuczkow@p.lodz.pl

The rather restrictive condition $r < r_c$ for the existence of PST deformations does not need to be satisfied if the nematic exhibits sufficiently strong flexoelectric properties. In such case, the periodic deformations arise in materials with typical values of r. They were observed by Vistin in planar untwisted layers and are called Vistin domains or longitudinal domains [28–32]. They appear at threshold voltages lower than the voltages for homogeneous deformations [33–39]. Flexoelectricity influences the director distribution; therefore the Vistin domains differ from the PST stripes. Flexoelectric properties also favor arising of the periodic deformations in twisted layers [40] in which they could not exist in the absence of flexoelectricity.

The present paper is devoted to numerical investigations of the periodic deformations induced in homogeneous planar and twisted layers containing a nematic liquid crystal possessing flexoelectric properties. They are interesting because flexoelectricity can become an essential feature of nematic mixtures containing mesogenic substances composed of bent-core molecules which exhibit giant flexoelectric properties [41,42]. Our aim was to recognize the structure of distorted layers and evolution of deformations during changes of bias voltage. The results show that the periodically deformed structures are related with lower free energy than the one-dimensional deformations; therefore they should be expected if the nematic mixture possesses sufficiently strong flexoelectric properties.

In Sec. II the parameters of the system under investigation are specified and the method of calculations is briefly described. The results are presented in Sec. III. Section IV contains a brief account of the results and a discussion.

II. ASSUMPTIONS AND METHOD

The nematic layers of thickness d confined between two electrodes parallel to the xy plane of the Cartesian coordinate system positioned at $z = \pm d/2$ were considered. The two-dimensional deformations of director distributions were taken into account. We assumed that all the physical quantities and variables describing the two-dimensional structures depended on two coordinates, y and z, and were constant along the x axis; i.e., the stripes were parallel to the x axis. The director distribution $\mathbf{n}(y,z)$ was determined by means of the polar angle $\theta(y,z)$ measured between $\mathbf{n}$ and the xy plane and by the azimuthal angle $\phi(y,z)$ between the x axis and the projection of $\mathbf{n}$ on the xy plane. The voltages U applied between the electrodes did not exceed values at which electroconvection could be expected in real experiments. The lower electrode was earthed. Boundary conditions were given by the polar and azimuthal angles θ_{s1}, θ_{s2}, ϕ_{s1}, and ϕ_{s2} which determined orientation of the easy axes $\mathbf{e_1}$ and $\mathbf{e_2}$ on the lower and upper electrode, respectively. The surface tilt angles $\theta_{s1} = \theta_{s2} = 0^\circ$ were imposed. The twist angle $\Phi = \phi_{s2} - \phi_{s1} = 90^\circ$ ensured the right-hand twist in the twisted layers, whereas $\Phi = 0^\circ$ corresponded to the untwisted planar layers. The anisotropic surface anchoring was assumed. The anisotropy was manifested by the difference between polar and azimuthal anchoring strengths. The anchoring energy was expressed by the formula proposed in [43,44] [see Eq. (1) below]. The anchoring strength parameters were constant in all the computations: $W_{\theta 1} = W_{\theta 2} = 10^{-4}\,\mathrm{J\,m^{-2}}$ and $W_{\phi 1} = W_{\phi 2} = 10^{-5}\,\mathrm{J\,m^{-2}}$. The thickness of the layers, $d = 5\,\mu$m, was also constant. Several sets of the elastic constants k_{11},k_{22},k_{33} were used corresponding to calamitic nematics and to mixtures of calamitic with bent-core compounds [45]. The saddle-splay elastic constant k_{24} was assumed to be zero. The flexoelectric coefficient e_{33} was varied between zero and 50 pC/m whereas $e_{11} = 0$ was assumed, which reflected approximately the properties of nematics composed of bent-core molecules. The dielectric anisotropy $\Delta\varepsilon = 2$ was adopted in all cases in order to simulate a mixture containing the bent-core nematics which exhibit small positive or negative values [45]. An additional advantage was that such small dielectric anisotropy weakly influenced the effects of a flexoelectric nature which were our main interest. The presence of ions was neglected; i.e., the nematic was treated as a perfect insulator.

The equilibrium structures of the director field inside the layer were determined by minimization of the free energy per unit area of the layer. For this purpose, we used the method which was successfully applied in earlier works [19,22,27]. A single stripe was considered during the computations. It was described by the director orientation angles θ and ϕ, the width λ and the angle ψ which the stripe made with the average direction of the easy axes $\mathbf{e} = (\mathbf{e_1} + \mathbf{e_2})/|\mathbf{e_1} + \mathbf{e_2}|$. The periodic boundary conditions along the y axis were imposed. The discrete angles θ_{ij} and ϕ_{ij} describing the director distribution over the cross section of the stripe as well as the electric potential V_{ij} were defined in the sites of the $M\times N$ regular lattice where $M = N = 256$. The indices $i = 1\cdots M$ and $j = 1\cdots N$ determined the position along the y and z axes, respectively. The coordinates $y = 0$ and $y = \lambda$ corresponded to $i = 1$ and $i = M$ whereas $z = -d/2$ and $z = d/2$ were labeled by $j = 1$ and $j = N$. The planes determined by $i = \mathrm{const}$ and $j = \mathrm{const}$ divided the cross section of the stripe into $(M-1)\times(N-1)$ rectangular cells. The values θ_{ij},ϕ_{ij}, and V_{ij} taken from the corners of each cell gave the average angles as well as the spatial derivatives of the angles and of the potential. They were used to calculate the total free energy counted per unit length of the stripe in the x direction. Then it was divided by λ in order to obtain the total free energy per unit area of the layer according to the formula

$$F = \frac{1}{2\lambda}\int_0^\lambda \left(\int_{-d/2}^{d/2} \{k_{11}(\nabla\mathbf{n})^2 + k_{22}[\mathbf{n}\cdot(\nabla\times\mathbf{n})]^2 + k_{33}[\mathbf{n}\times(\nabla\times\mathbf{n})]^2 - 2(k_{22}+k_{24})\nabla[\mathbf{n}\cdot(\nabla\mathbf{n}) + \mathbf{n}\times\nabla\times\mathbf{n}]$$
$$- 2[e_{11}\mathbf{n}\cdot\nabla\mathbf{n} - e_{33}\mathbf{n}\times(\nabla\times\mathbf{n})]\cdot\mathbf{E} - \varepsilon_0\varepsilon_\perp E^2 - \varepsilon_0\Delta\varepsilon(\mathbf{n}\cdot\mathbf{E})^2\}\mathrm{d}z\Big)\mathrm{d}y + \frac{1}{2\lambda}\int_0^\lambda \{[W_{\varphi 1}\cos^2(\theta_1-\theta_{s1}) + W_{\theta 1}\sin^2(\theta_1-\theta_{s1})]$$
$$\times[1-(\mathbf{n_1}\cdot\mathbf{e_1})^2]\}\mathrm{d}y + \frac{1}{2\lambda}\int_0^\lambda \{[W_{\varphi 2}\cos^2(\theta_2-\theta_{s2}) + W_{\theta 2}\sin^2(\theta_2-\theta_{s2})][1-(\mathbf{n_2}\cdot\mathbf{e_2})^2]\}\mathrm{d}y, \quad (1)$$

where $\mathbf{n_1}$,$\mathbf{n_2}$ denote the directors adjacent to the lower and upper plate, respectively, whereas θ_1 and θ_2 are their polar orientation angles. This energy was minimized with respect to all the angles θ_{ij} and ϕ_{ij}, spatial period λ, and the angle ψ. Initially, the values $\theta_{ij} = 0$ and $\phi_{ij} = (\pi/2)(j-1)/(N-1)$, where $i = 1 \cdots M$ and $j = 1 \cdots N$, were introduced (according to the uniform twisted initial director orientation imposed by the easy axes). The initial distribution of the electric potential corresponding to uniform electric field was assumed, $V_{ij} = U(j-1)/(N-1)$. The initial value of the angle ψ was determined by the easy axes whereas $\lambda = d$ was adopted. The final set of the variables θ_{ij},ϕ_{ij},λ, and ψ, which approximated the real equilibrium director distribution, was calculated in the course of an iteration process. During the computations, the values of θ_{ij},ϕ_{ij},λ, and ψ were varied successively by small intervals. The free energy per unit area of the layer was calculated after each change. If the new energy was lower than the previous one, the changed value of the variable was accepted and the corresponding interval was increased by a factor of about 1.5. In the opposite case, the variable remained unchanged and the interval was decreased to about 0.8 of its previous value. When the new values of angles in all sites of the lattice as well as the new values of λ and ψ were found, the electric potential distribution $V(y,z)$ in the layer was calculated. For this purpose the Poisson equation

$$\begin{aligned}
&\varepsilon_0\left[\frac{\partial V}{\partial y}\left(\frac{\partial \varepsilon_{yy}}{\partial y}+\frac{\partial \varepsilon_{yz}}{\partial z}\right)+\frac{\partial V}{\partial z}\left(\frac{\partial \varepsilon_{yz}}{\partial y}+\frac{\partial \varepsilon_{zz}}{\partial z}\right)+\varepsilon_{yy}\frac{\partial^2 V}{\partial y^2}+2\varepsilon_{yz}\frac{\partial^2 V}{\partial y\partial z}+\varepsilon_{zz}\frac{\partial^2 V}{\partial z^2}\right]-e_{11}\left(\frac{\partial n_y}{\partial y}+\frac{\partial n_z}{\partial z}\right)^2\\
&-e_{11}n_y\left(\frac{\partial^2 n_y}{\partial y^2}+\frac{\partial^2 n_z}{\partial y\partial z}\right)-e_{11}n_z\left(\frac{\partial^2 n_y}{\partial y\partial z}+\frac{\partial^2 n_z}{\partial z^2}\right)+e_{33}\left(\frac{\partial n_z}{\partial y}r_x+n_z\frac{\partial r_x}{\partial y}-\frac{\partial n_x}{\partial y}r_z-n_x\frac{\partial r_z}{\partial y}\right)\\
&+e_{33}\left(\frac{\partial n_x}{\partial z}r_y+n_x\frac{\partial r_y}{\partial z}-\frac{\partial n_y}{\partial z}r_x-n_y\frac{\partial r_x}{\partial z}\right)=0 \qquad (2)
\end{aligned}$$

was resolved, where $r_x = \partial n_z/\partial y - \partial n_y/\partial z$, $r_y = \partial n_x/\partial z$, $r_z = -\partial n_x/\partial y$; n_i and ε_{ij} are components of the director and of the dielectric permittivity tensor. The boundary conditions $V(-d/2) = 0$ and $V(d/2) = U$ were imposed where $U > 0$. As a result, the values of potential in the sites of the lattice, V_{ij}, were obtained. In this way a single cycle of computations was finished and resulted in the new set of variables suitable for the next cycle. The cycles were repeated until further reduction in the total free energy could be neglected. As a result, a state of minimum energy was obtained.

We estimate the numerical errors in the director orientation angles to be less than 5° and in the threshold voltages to be less than 0.1 V.

III. RESULTS

A. Untwisted planar layers

Spatially periodic deformations in untwisted planar layers arise without the contribution of flexoelectricity (for instance, under the action of magnetic field [10]) provided that the ratio $r = k_{22}/k_{11}$ is smaller than $r_c = 0.303$, which is rather rare. They are known as the PST stripes. The periodic structure of them can be characterized by the first Fourier components of the functions describing the dependencies of θ and ϕ on y and z:

$$\begin{aligned}
\theta(y,z) &\propto \cos(\pi z/d)\sin(2\pi y/\lambda),\\
\phi(y,z) &\propto \cos(2\pi z/d)\cos(2\pi y/\lambda). \qquad (3)
\end{aligned}$$

If the nematic material possesses flexoelectric properties then the electric field applied to the layer induces periodic deformations also in the case of typical relations between elastic constants, i.e., if $r > r_c$. They take the form of Vistin domains [28]. Symmetry of their internal structure differs from the PST symmetry expressed by Eq. (3) because of the complex action of surface and bulk flexoelectric torques. Our calculations showed that if the flexoelectric properties were sufficiently strong, the corresponding functions were

$$\begin{aligned}
\theta(y,z) &\propto \cos(\pi z/d)\sin(2\pi y/\lambda),\\
\phi(y,z) &\propto \cos(\pi z/d)\cos(2\pi y/\lambda), \qquad (4)
\end{aligned}$$

instead of (3) [39]. In order to illustrate the transition from (3) to (4) we performed simulations assuming $r = 0.2$ and using several values of e_{33}. The results showing evolution from PST stripes to Vistin domains are presented symbolically in Fig. 1.

They show that the change of symmetry was realized continuously when the flexoelectric properties were gradually enhanced. This effect reveals the relationship between Vistin domains and PST patterns.

In the following, we report results of computations performed for some model liquid crystalline material characterized by elastic constant ratios typical for calamitic nematics: $k_{11} = 10\,\mathrm{pN}, k_{22} = 5\,\mathrm{pN}, k_{33} = 15\,\mathrm{pN}$. Initial homogeneous director distribution was determined by $\theta(y,z) = 0$ and $\phi(y,z) = 0$. Under the action of external electric field, the periodic deformations arose continuously with finite initial spatial period if the threshold voltage U_1 was exceeded. They can be recognized as longitudinal Vistin domains [28]. Energy per unit area of the periodically deformed layer was lower than the energy of homogeneous deformation which would arise under the same circumstances. In Fig. 2 the structure of

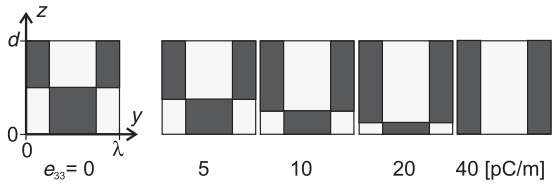

FIG. 1. Schematic distributions of signs of $\phi(y,z)$ in the cross sections of stripes illustrating the influence of flexoelectricity on the structure of deformed layers. Dark and bright regions correspond to negative and positive angles ϕ, respectively. $r = 0.2$. Values of e_{33} (in pC/m) are given.

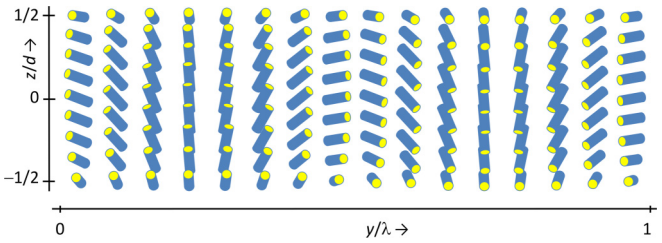

FIG. 2. Director field in the cross section of a single stripe arising in planar layer; $e_{33} = 20\,\mathrm{pC/m}$; $U = 3\,\mathrm{V}$.

a single stripe at a moderate voltage is illustrated by means of cylinders symbolizing the directors, oriented according to calculated values of θ_{ij} and ϕ_{ij}. Four parts can be distinguished in the stripe according to the symmetry determined by Eq. (4). They differ in signs of the angles θ and ϕ: $\theta > 0$ and $\phi < 0$; $\theta > 0$ and $\phi > 0$; $\theta < 0$ and $\phi > 0$; $\theta < 0$ and $\phi < 0$.

The deformations grew with increasing voltage. This process is illustrated in Fig. 3 by means of the quantity Θ which plays the role of amplitude of the function $\theta(y,0)$, defined as $\Theta = (\theta_{\max} - \theta_{\min})/2$ where $\theta_{\max}$ and $\theta_{\min}$ are the maximum and minimum values of $\theta(y,0)$, respectively. Development of deformations is illustrated in Fig. 4 by means of the width of the stripes plotted as a function of voltage.

If the flexoelectric parameter was relatively small (e.g., if $e_{33} = 10\,\mathrm{pC/m}$) then the stripes slightly narrowed with increasing voltage. At sufficiently large voltage, two halves of the stripe could be distinguished. In each of them, the deformation represented by the angle θ dominated, whereas the twist deformation described by the angle ϕ was weak and limited to narrow regions on the boundaries between the halves. As a result, the director distributions in each half became similar to the distributions occurring in homogeneous deformations. Finally, the spatial period diverged rapidly to infinity when some critical voltage U_2 was reached, which means that the homogeneous deformation spread over the whole area of the layer and replaced the periodic patterns. In the case of strong flexoelectricity (e.g., if $e_{33} = 50\,\mathrm{pC/m}$) the stripes narrowed steadily with increasing voltage which agrees

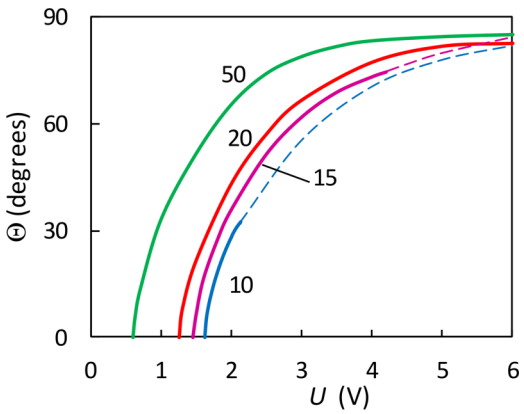

FIG. 3. Amplitude Θ of deformations arising in planar layers as a function of bias voltage U. Solid lines: periodic patterns; dashed lines: homogeneous deformations. Values of e_{33} (in pC/m) are indicated at the curves.

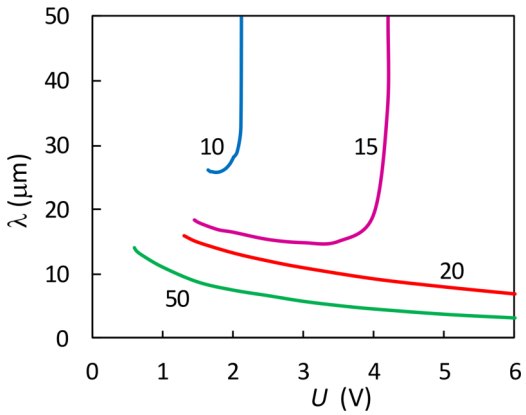

FIG. 4. Spatial period λ of deformations arising in planar layers as a function of bias voltage U. Values of e_{33} (in pC/m) are indicated at the curves.

with experimental data presented in [46]. The corresponding wave number $q = 2\pi/\lambda$ was a linearly increasing function of voltage. No transition to one-dimensional deformation was observed up to $U = 10\,\mathrm{V}$. (Higher voltages were not taken into account because we expect that in a real experiment they would induce electrohydrodynamic instabilities.)

B. Twisted layers of typical calamitic nematics

In the following, the periodic patterns in the twisted nematic layers characterized by the angle $\Phi = 90^\circ$ are described. The elastic constants and other parameters of nematics were the same as in the homogeneous planar case. The actual twist angles of the director field, $\Delta\phi(y) = \phi(y,d/2) - \phi(y,-d/2)$, were slightly smaller than Φ because of finite azimuthal anchoring strength.

In all the cases, deformations arose at some threshold voltage U_1 with amplitude Θ starting from zero (Fig. 5). They had the form of stripes with finite width which were directed at some acute angle ψ with respect to the unit vector

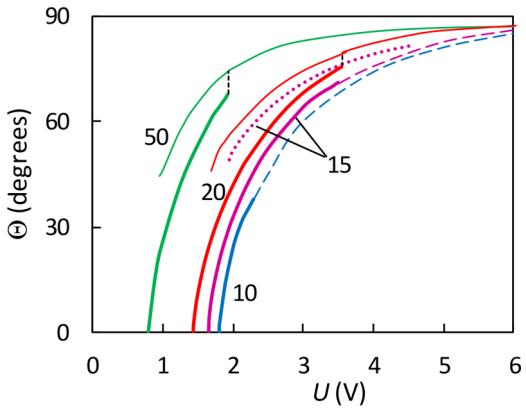

FIG. 5. Amplitude Θ of deformations arising in twisted layers as a function of bias voltage U. Thick lines: type 1 patterns; thin lines: type 2 patterns; dashed lines: homogeneous deformations. Dashed vertical lines indicate rapid changes of the type of deformations. Dotted line denotes the energetically unfavorable deformation of type 2. Values of e_{33} (in pC/m) are indicated at the curves.

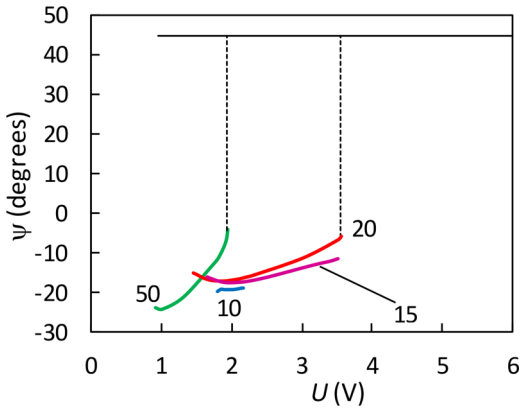

FIG. 6. Direction of stripes arising in twisted layers determined by the angle ψ as a function of bias voltage U. Thick lines: type 1 patterns; thin line at $\psi = 45^\circ$ corresponds to the type 2 patterns for $e_{33} = 20$ and 50 pC/m. Dashed lines indicate rapid change of the type of deformations at $U = U_3$. Values of e_{33} (in pC/m) are indicated at the curves.

e (Fig. 6). We use the name "type 1" patterns for them. They can be identified as the domains observed by Umanski *et al.* [40]. The threshold as well as the width of the initial stripes decreased when the flexoelectric properties became stronger (Fig. 7). The exemplary structure of the stripe is shown in Fig. 8. The escaped disclination of strength 1 is created in the vicinity of the negative electrode where $\theta = 0$ and $\phi = 0$ simultaneously.

In the case of weak flexoelectricity, e.g., when $e_{33} = 10$ pC/m or $e_{33} = 15$ pC/m, the angle ψ was nearly constant (Fig. 6). The deformations evolved in a way similar to the untwisted case (Fig. 5). Two halves were formed as a result of increasing voltage. The director distributions in each half tended to the distributions occurring in one-dimensional deformations. The stripes of type 1 existed up to some critical voltages U_2 above which their width became infinite, as shown in Fig. 7, and the homogeneous deformations appeared.

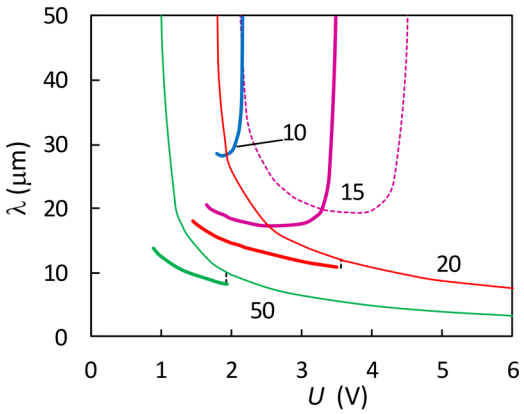

FIG. 7. Spatial period λ of deformations arising in twisted layers as a function of bias voltage U. Thick lines: type 1; thin lines: type 2. Dashed vertical lines indicate rapid change of the type of deformations at $U = U_3$. Dotted line denotes the energetically unfavorable deformation of type 2. Values of e_{33} (in pC/m) are indicated at the curves.

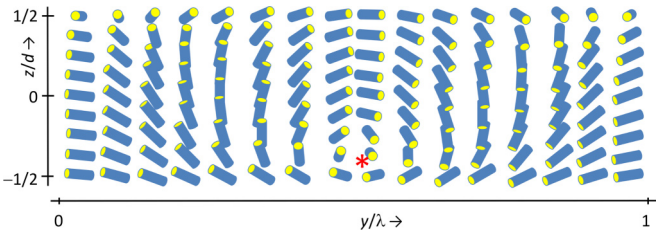

FIG. 8. Director field in the cross section of a single stripe of type 1 occurring in the twisted layer. The star indicates position of the escaped disclination line. $e_{33} = 20$ pC/m; $U = 3$ V.

In the case of stronger flexoelectricity, represented by $e_{33} = 20$ pC/m or $e_{33} = 50$ pC/m, the deformations grew continuously with increasing voltage. Simultaneously, the width of the stripes decreased monotonically and their direction determined by the angle ψ varied. At some voltage U_3, the structure of the stripes changed discontinuously due to reorientation of director distribution which was manifested by jumps of Θ, λ, and ψ as functions of voltage. In particular, the angle ψ adopted the constant value of 45°. In the following, these domains are called type 2 patterns. Calculations revealed that the free energy of deformations decreased during transition from type 1 to type 2 occurring at U_3. The structure of this type is shown in Fig. 9. Two moderately distorted halves bounded by narrow regions of stronger deformation can be distinguished. Above U_3, the type 2 deformation strengthened. The amplitude Θ increased further with increasing voltage. Simultaneously the stripes narrowed, with linearly increasing wave number. However, when the voltage was decreased below U_3, no return to the structure of type 1 was observed. The stripes retained their direction at $\psi = 45^\circ$ which gave rise to the occurrence of some kind of hysteretic behavior. The deformations in the halves of the stripes weakened; i.e., the director distributions tended to the undistorted state. However, in the regions near the boundaries between the halves, the angles θ adopted quite significant values which gave rise to large amplitudes Θ shown in Fig. 5. Simultaneously, the spatial period increased and diverged to infinity at another critical voltage U_4. Just below U_3, the energy of the type 2 deformation was lower than that of type 1; however, this relation became reversed at some lower voltage, so the type 2 patterns became energetically unfavorable. Nevertheless, the type 2 stripes may occur down to U_4 according to the so-called perfect delay principle, which explains that that the state of a system remains at the local minimum of a potential as long as that minimum exists [47].

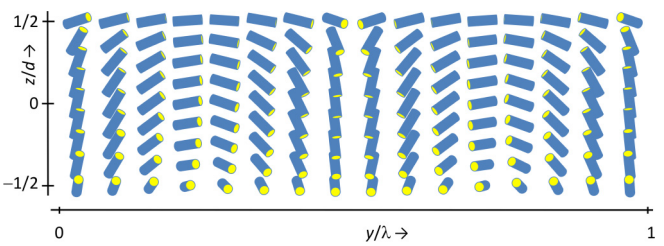

FIG. 9. Director field in the cross section of a single stripe of type 2 occurring in the twisted layer. $e_{33} = 20$ pC/m; $U = 3$ V.

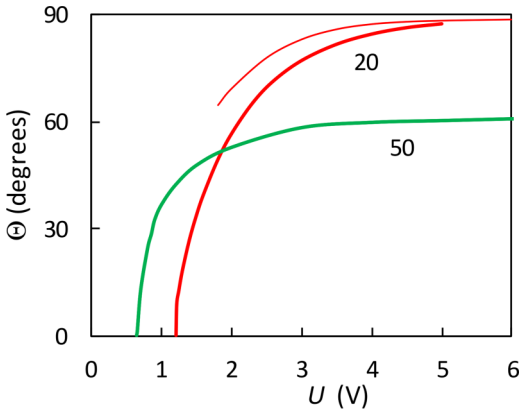

FIG. 10. Amplitude Θ of periodic patterns arising in twisted layers containing mixture A as a function of bias voltage U. Thick lines: type 1 patterns; thin line: type 2 patterns. Values of e_{33} (in pC/m) are indicated at the curves.

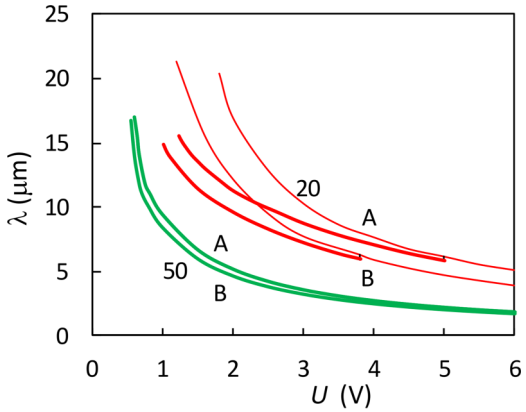

FIG. 12. Spatial period of deformations arising in twisted layers containing mixtures A and B as a function of bias voltage U. Thick lines: type 1 patterns; thin lines: type 2 patterns. Values of e_{33} (in pC/m) are indicated at the curves.

The patterns of type 2 were found also if $e_{33} = 15\,\mathrm{pC/m}$ which is illustrated by the dotted curves in Figs. 5 and 6. However, they had larger energy than type 1 and were not available when the voltage applied to the undisturbed layer was increased from zero.

C. Twisted layers of mixtures containing bent-core nematics

Strong flexoelectric properties can be obtained in mixtures containing nematic substances composed of bent-core molecules. In this section, we describe deformations occurring in the model mixtures of this kind. The bent-core nematics have peculiar elastic properties manifested by the specific relation between elastic constants: $k_{11} > k_{33} > k_{22}$. For this reason we performed exemplary calculations using two sets of elastic constants: $k_{11} = 8\,\mathrm{pN}$, $k_{22} = 3\,\mathrm{pN}$, $k_{33} = 10\,\mathrm{pN}$ and $k_{11} = 7\,\mathrm{pN}$, $k_{22} = 2\,\mathrm{pN}$, $k_{33} = 7\,\mathrm{pN}$, which simulated two mixtures of calamitic and bent-core nematics denoted A and B, respectively.

The results for both mixtures were qualitatively the same as those found for calamitic nematics. The deformations started as the stripes of type 1 and grew with increasing voltage as shown in Figs. 10 and 11. Simultaneously the spatial period narrowed while the wave number was a linear function of voltage (Fig. 12). In the case of $e_{33} = 20\,\mathrm{pC/m}$, they were transformed into the stripes of type 2 when the voltage achieved a suitable value. The type 2 patterns were retained when the voltage was lowered. In the case of stronger flexoelectricity, e.g., if $e_{33} = 50\,\mathrm{pC/m}$, no transition to the type 2 patterns was detected up to $U = 10\,\mathrm{V}$. Figure 13 presents smooth changes of direction of the type 1 stripes and switching to type 2 for which $\psi = 45^\circ$.

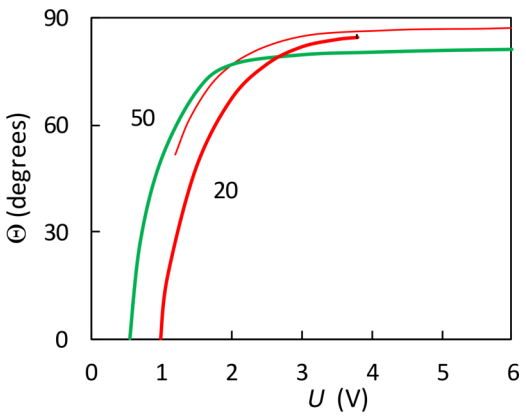

FIG. 11. Amplitude Θ of periodic patterns arising in twisted layers containing mixture B as a function of bias voltage U. Thick lines: type 1 patterns, thin line: type 2 patterns. Values of e_{33} (in pC/m) are indicated at the curves.

IV. SUMMARY AND DISCUSSION

Electric field induced deformations in twisted and untwisted planar layers of nematic liquid crystals possessing flexoelectric properties were investigated. It was found that the spatially periodic deformations, taking the form of parallel stripes, were due to smaller free energy than the homogeneous deformations. The relations between free energies due to

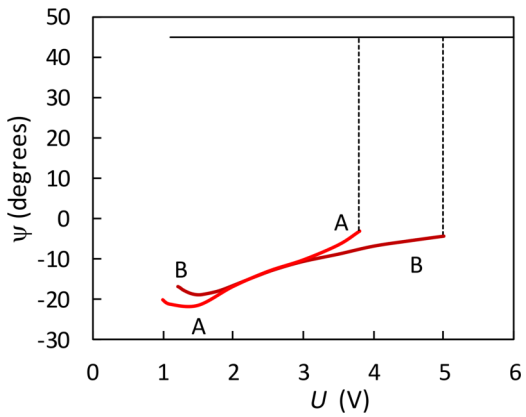

FIG. 13. Direction of the type 1 stripes of deformations arising in twisted layers containing mixtures A and B of calamitic and bent-core nematics as a function of bias voltage U. Thick lines: type 1 patterns; thin line: type 2 patterns. Dashed vertical lines indicate rapid change of the type of deformations at $U = U_3.e_{33} = 20\,\mathrm{pC/m}$.

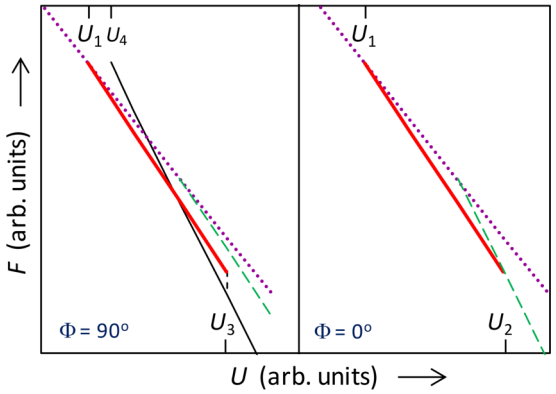

FIG. 14. Schematic presentation of the free energies per unit area of the layer related to different types of deformations plotted as functions of voltage. Left part: twisted layers; right part: planar layers. Dotted lines: undistorted state; dashed lines: one-dimensional deformation; thin solid line: type 2 patterns; thick lines: type 1 patterns in twisted case and periodic pattern in planar layer. Voltages $U_1 \cdots U_4$ correspond to changes of the kind of deformations.

different types of deformations are shown schematically in Fig. 14.

The structures of the stripes differed from the form of patterns induced by magnetic field [10,20,22] which is a consequence of the dominating role of the flexoelectric torques over the dielectric torques. The periodic deformations seem to be common if flexoelectricity has significant magnitude.

In the untwisted planar layers the stripes were parallel to the initial director orientation. At sufficiently high voltage U_2 their spatial period increased to infinity; i.e., the stripes were transformed into the homogeneous deformations. In the case of strong flexoelectricity, voltage U_2 exceeded values at which the electroconvection could be expected.

In the twisted layers, two different kinds of deformations were distinguished, called here type 1 and type 2 patterns. The stripes of type 1 were directed at some acute angle with respect to the unit vector **e**. In the case of weak flexoelectricity they widened to infinity at some critical voltage and were replaced by homogeneous deformations. In the case of strong flexoelectricity, the stripes narrowed until some voltage U_3 was achieved at which a rapid change to the type 2 patterns occurred. The stripes of type 2 made the angle 45° with respect to the unit vector **e**. This transition was connected with the reorientation of director distribution which led to lower energy. It resulted in arising of the subtle equilibrium between elastic, dielectric, and flexoelectric torques acting in the bulk and torques due to flexoelectricity and anchoring acting on the boundary surfaces. The structure developed with increasing voltage. However, when the voltage decreased below U_3, some kind of hysteretic behavior occurred; i.e., the patterns of type 2 were retained. The type 1 deformation was not restored. Instead, the deformation of type 2 weakened while its spatial period diverged to infinity at another critical voltage U_4 which means that the director distribution tended to the undistorted state.

Additional preliminary computations with anchoring strengths $W_{\theta 1}$, $W_{\theta 2}$, $W_{\phi 1}$, and $W_{\phi 2}$ enhanced or reduced by a factor of 2 with respect to our main values showed that the evolution of the patterns during changes of voltage was qualitatively the same as illustrated in Figs. 3–7. The threshold voltages $U_1 \cdots U_4$ increased when the anchoring became stronger and decreased when the surface interactions were weaker.

The stronger the flexoelectric properties were, the wider was the range of voltages at which the type 1 patterns existed. It was also wider in the case of mixtures containing bent-core nematics. The positive values of e_{33} were used during all calculations. Additional calculations showed that if $e_{33} < 0$ was adopted, then the stripes symmetrical with respect to the midplane of the layer and oriented at the angle ψ of opposite sign were obtained. The same effect was obtained if $\Phi = -90^\circ$ was adopted or if the sign of voltage was reversed, which agrees with the experiment reported in [40].

The results concerning the type 1 patterns as well as those obtained for the planar layers also agree with experimental observations [28,40,46]. The type 2 patterns should be searched in layers containing nematics with sufficiently strong flexoelectricity.

[1] D.-K. Yang and S.-T. Wu, *Fundamentals of Liquid Crystal Devices* (John Wiley & Sons, New York, 2014).

[2] R. B. Meyer, Phys Rev Lett. **22**, 918 (1969).

[3] L. M. Blinov, *Structure and Properties of Liquid Crystals* (Springer, New York, 2010).

[4] L. M. Blinov and V. G. Chigrinov, *Electrooptic Effects in Liquid Crystal Materials* (Springer, Berlin, Heidelberg, 1994).

[5] B. Jérôme, in *Handbook of Liquid Crystals*, edited by D. Demus, J. Goodby, G.W. Gray, H.-W. Spiess, and V. Vill (Wiley, New York, 1998), Vol. 1, p. 535.

[6] L. Kramer and W. Pesch, in *Physical Properties of Liquid Crystals: Nematics*, edited by D. A. Dunmur, A. Fukuda, and G. R. Luckhurst (Inspec, London, 2001), pp. 441–454.

[7] H. P. Hinov, I. Bivas, M. D. Mitov, K. Shoumarov, and Y. Marinov, Liq. Cryst. **30**, 1293 (2003).

[8] *Flexoelectricity in Liquid Crystals. Theory, Experiments and Applications*, edited by Á. Buka and N. Éber (Imperial College Press, London, 2012).

[9] A. Krekhov, W. Pesch, and Á. Buka, Phys. Rev. E **83**, 051706 (2011).

[10] F. Lonberg and R. B. Meyer, Phys. Rev. Lett. **55**, 718 (1985).

[11] U. D. Kini, J. Phys. (Paris) **47**, 693 (1986).

[12] E. Miraldi, C. Oldano, and A. Strigazzi, Phys. Rev. A **34**, 4348 (1986).

[13] U. D. Kini, J. Phys. (Paris) **47**, 1829 (1986).

[14] H. M. Zenginoglu, J. Phys. (Paris) **48**, 1599 (1987).

[15] G. Barbero, E. Miraldi, and C. Oldano, Phys. Rev. A **38**, 519 (1988).

[16] U. D. Kini, J. Phys. (Paris) **51**, 529 (1990).

[17] G. Derfel, Liq. Cryst. **11**, 431 (1992).

[18] A. Sparavigna and A. Strigazzi, Mol. Cryst. Liq. Cryst. **254**, 209 (1994).
[19] D. Krzyżański and G. Derfel, Phys. Rev. E **61**, 6663 (2000).
[20] U. D. Kini, J. Phys. (Paris) **48**, 1187 (1987).
[21] P. Schiller, Phase Trans. **29**, 59 (1990).
[22] D. Krzyżański and G. Derfel, Liq. Cryst. **29**, 951 (2002).
[23] D. Krzyżański and G. Derfel, Proc. SPIE **4759**, 237 (2002).
[24] V. I. Tsoy, G. V. Simonenko, and V. G. Chigrinov, Liq. Cryst. **13**, 227 (1993).
[25] M. Akatsuka, K. Katoh, K. Sawada, and M. Nakayama, Proc. Soc. Inf. Display **28**, 59 (1987).
[26] T. Scheffer and J. Nehring, Annu. Rev. Mater. Sci. **27**, 555 (1997).
[27] D. Krzyżański and G. Derfel, J. Appl. Phys. **95**, 3535 (2004).
[28] L. K. Vistin, Sov. Phys. Crystallogr. **15**, 514 (1970).
[29] M. I. Barnik, L. M. Blinov, A. N. Trufanov, and B. A. Umanski, Sov. Phys., J. Exper. Theor. Phys. **46**, 1016 (1977).
[30] P. Schiller, G. Pelzl, and D. Demus, Cryst. Res. Technol. **25**, 111 (1990).
[31] Y. Marinov, H. P. Hinov, and A. G. Petrov, J. Optoelectron. Adv. Mater. **7**, 277 (2005).
[32] P. Kumar and K. S. Krishnamurthy, Liq. Cryst. **34**, 257 (2007).
[33] S. G. Dmitriev, Sov. Phys., J. Exper. Theor. Phys. **34**, 1093 (1972).
[34] Y. P. Bobylev and S. A. Pikin, Sov. Phys., J. Exper. Theor. Phys. **45**, 195 (1977).
[35] Y. P. Bobylev, V. G. Chigrinov, and S. A. Pikin, J. Phys. Colloq. **40**, C3-331 (1979).
[36] S. A. Pikin, *Structural Transformations in Liquid Crystals* (Gordon and Breach, New York, 1991).
[37] I. Lelidis and G. Barbero, Phys. Lett. A **311**, 242 (2003).
[38] M. Ledney and I. Pinkevych, Liq. Cryst. **34**, 577 (2007).
[39] G. Derfel and M. Buczkowska, Mol. Cryst. Liq. Cryst. **547**, 213 (2011).
[40] B. A. Umanski, V. G. Chigrinov, L. M. Blinov, and Yu. B. Podyachev, Sov. Phys., J. Exper. Theor. Phys. **54**, 694 (1981).
[41] J. Harden, B. Mbanga, N. Éber, K. Fodor-Csorba, S. Sprunt, J. T. Gleeson, and A. Jákli, Phys. Rev. Lett. **97**, 157802 (2006).
[42] A. Jákli, Liq. Cryst. Rev. **1**, 65 (2013).
[43] G. Derfel and M. Buczkowska, Liq. Cryst. **42**, 1213 (2015).
[44] G. Derfel and M. Buczkowska, Sci. Bull. Lodz Univ. Technol., Phys. **36**, 5 (2015).
[45] S. Kaur, Liq. Cryst. **43**, 2277 (2016).
[46] N. Éber, P. Salamon, and Á. Buka, Liq. Cryst. Rev. **4**, 101 (2016).
[47] T. Poston and I. Stewart, *Catastrophe Theory and Its Applications*, Surveys and Reference Works in Mathematics Vol. 2 (Pitman, London, 1978).